PROCEEDINGS OF SCIENCE

The Infrared Phase of QCD and Anderson Localization

Ivan Horváth[a,b,*]

[a] *Nuclear Physics Institute CAS,*
Hlavní 130, 25068 Řež (Prague), Czech Republic
[b] *Department of Physics and Astronomy, University of Kentucky,*
506 Library Drive, Lexington KY 40506, USA
[c] *Department of Physics, The George Washington University,*
725 21st St. NW, Washington DC 20052, USA

E-mail: horvath@ujf.cas.cz

When Anderson localization entered the QCD landscape, it was almost immediately thought about in connection with thermal phases, namely as a factor in the chiral phase transition or crossover. However, recent developments revealed an additional structure that made Anderson-like features central to the genesis and understanding of the new thermal phase: the IR phase of QCD. I will explain these developments.

The XVIth Quark Confinement and the Hadron Spectrum Conference (QCHSC24)
19-24 August, 2024
Cairns Convention Centre, Cairns, Queensland, Australia

*Speaker

 ISSN 1824-8039 . Published by SISSA Medialab.

PoS(QCHSC24)054

1. Introduction

In this talk I will describe what is shaping up as a new case of fruitful cross-fertilization between elementary particle and condensed matter physics. On the former side it involves a recent development, namely the unexpected finding of a new thermal regime in QCD [1–4], characterized by proliferation of deeply infrared ($0 \lesssim \lambda \ll T$) Dirac modes, decoupling of the infrared physics (IR-bulk separation), and scale invariant glue in the ensuing IR component. This new regime is known as the *IR phase* and is interesting not only due to the novel nature of its thermal state but also due to the fact that the associated change may be a true phase transition occurring at temperature $T_{\rm IR}$ ($200\,{\rm MeV} < T_{\rm IR} < 230\,{\rm MeV}$) just above the known range of crossover temperatures.

On the other side of the above relationship is the time-honored phenomenon of Anderson localization, namely the exponential pinning of a quantum particle by virtue of spatial disorder [5, 6], which proved to have a significant impact on condensed matter physics and various applied areas. But its potential role in the fundamental physics, e.g. at the level of the Standard Model of elementary particles, was (and in some ways still is) barely considered in the literature. A fruitful remark in Ref. [7] suggested that, at sufficiently high temperatures, thermal fluctuations in the strong sector (QCD) may induce localization of quark modes in low-lying part of Dirac spectra. The associated loss of IR quark mobility then led to the suggestion that QCD chiral transition (massless limit), and by proxy the transition in real-world QCD, could be viewed as analogous to metal-to-insulator transition of Anderson-like type [8, 9]. Such considerations gained some traction when localization in hot QCD started to be investigated more systematically and the Anderson-like mobility edge $\lambda_{\rm A} > 0$ has been identified[1] at sufficiently high temperatures [10–12].

But contradictions soon appeared as well [2, 13]. To that end, note that the "insulating nature" of hot thermal state in metal-to-insulator scenario signifies the absence of long-distance ($\gtrsim 1/T$) physics. This was assumed to arise due to the infrared (IR) modes being localized at shorter scales, and due to the expected depletion of Dirac spectrum in this range. But chiral polarization properties of deep IR modes at high temperatures [13] and their strong proliferation contrary to expectations [2] suggested that IR physics is actually present, raising the possibility that metal-to-insulator scenario may not reflect some key aspects of QCD reality.

The above discord became sharp once the evidence for IR phase was presented and its defining features were laid down in Ref. [1]. While in this original work it was already anticipated that the mobility edge $\lambda_{\rm A} \neq 0$ is the key element for the proposed IR-bulk separation, and that the non-analyticity introduced by it shields the IR from renormalization-group running in line with its observed scale invariance, the nature of this IR physics remained foggy from the model point of view. After all, this aspect wasn't even present in the metal-to-insulator scenario. The crucial step in this regard occurred in Ref. [3] which studied effective spatial dimensions of IR modes and, apart from intriguing non-analytic (in λ) behavior suggesting topology at play, found out that $\lambda_{\rm IR} \equiv 0$ behaves in many ways similarly to the mobility edge $\lambda_{\rm A} \neq 0$. Subsequently, Ref. [4] provided evidence that $\lambda_{\rm IR} = 0$ is indeed a new Anderson-like mobility edge, and formulated the *metal-to-critical* scenario of transition to IR phase based on both edges.

[1]Note that in this continuum notation, where non-zero Dirac eigenvalues come in conjugate pairs $\pm i\lambda$, we frequently only consider the upper branch $\lambda \geq 0$.

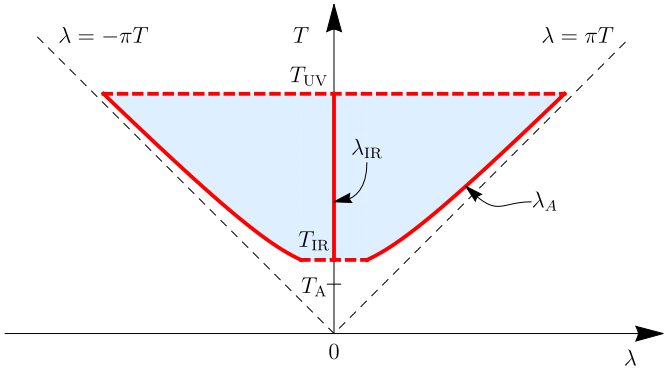

Figure 1: Phase diagram for Anderson-like properties in the Dirac spectrum of thermal QCD [4]. See the explanation in the text. Temperature $T_{\rm A}$ is the crossover point for Dirac spectral properties [1] and thin dashed lines the Matsubara scales.

The metal-to-critical scenario for QCD (and its novelty) is conveyed by the phase diagram for Anderson-like Dirac properties [4], shown in Fig. 1. Here the thick red lines in the $\lambda - T$ plane represent the Anderson-like critical points (mobility edges). Dashing at horizontal segment $T = T_{\rm IR}$ signifies that it may be of zero length (single point), while dashing at segment $T = T_{\rm UV}$ means that it may be pushed all the way to $T_{\rm UV} = \infty$. At each temperature $T_{\rm IR} < T < T_{\rm UV}$, when the system is in IR phase, there are critical points $\pm\lambda_{\rm A}$ and $\lambda_{\rm IR}$ in the Dirac spectrum, yielding the modes in the range $(-\lambda_{\rm A}, \lambda_{\rm IR}) \cup (\lambda_{\rm IR}, \lambda_{\rm A})$ (the blue inside region) localized with varying localization lengths that diverge at $\pm\lambda_{\rm A}$ and $\lambda_{\rm IR}$. The chief tenet of the relationship between the thermal state of QCD in IR phase and its Anderson-like representation (metal-to-critical picture) is that the above constellation of critical points captures the unusual features found in the former: the non-analyticity at $\lambda_{\rm A}$ facilitates the IR-bulk separation and protects the IR from renormalization-group running, while the criticality at $\lambda_{\rm IR}$ determines the nature of its long-range physics.

In this talk I will discuss the developments that led to the notion of IR phase and its current understanding in some detail. The goal is to describe them in a manner that brings to the fore the continued interrelationships of the process with the physics of Anderson localization.

2. IR Phase

The first major step toward the notion of IR phase was taken in Ref. [2]. The authors argued that a qualitatively new regime characterized by anomalously strong accumulation of IR Dirac modes exists in SU(3) gauge theories with fundamental quarks. They showed that this accumulation, observed in lattice-regularized theory, persists into the continuum limit and suggested that the ensuing IR degrees of freedom (dof's) decouple and defy confinement (partially deconfined phase).

While the proliferation of IR dof's remained the chief qualitative underpinning of the new regime, the notion of IR phase eventually arose from the revelation [1] that the effect is quantitatively expressed as a power-law (negative power) IR behavior of Dirac spectral density[2]. In fact, at least in thermal cases, the near-pure power $p = -1 + \delta$ with very small $\delta \geq 0$ was found. All basic tenets

[2]Recall that Dirac spectral density $\rho(\lambda)$ of the theory is the average number of Dirac eigenmodes per unit 4-volume and unit spectral interval in the infinitesimal neighborhood of λ.

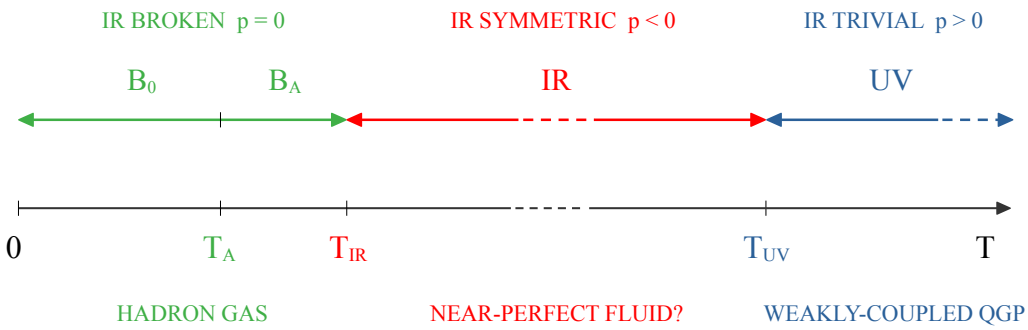

Figure 2: Types of phases in SU(3) gauge theories with fundamental quarks based on the abundance of deep-IR degrees of freedom and IR scale invariance. See the discussion in the text.

of IR phase were formulated in that work, and SU(3) gauge theories with fundamental quarks were classified into three qualitatively different types (phases) based on a degree of their Dirac mode accumulation in deep IR, namely [1]

$$\rho(\lambda) \propto \lambda^p \quad \text{for} \quad \lambda \to 0 \qquad \longrightarrow \qquad \text{phase} = \begin{cases} \text{B} & \text{if} \quad p = 0 \\ \text{IR} & \text{if} \quad p < 0 \\ \text{UV} & \text{if} \quad p > 0 \end{cases} \tag{1}$$

The names of phases are derived from the proposed relationship of IR glue to scale invariance: B is a shorthand for IR-Broken and corresponds to hadronic phase such as in real-world QCD at low temperatures.[3] IR refers to IR-Symmetric phase which is synonymous to the IR phase and for which a possible connection to near-perfect fluid medium observed at RHIC and LHC was raised [1]. UV dubs "IR-Trivial" since IR degrees of freedom are power-law suppressed. This regime would correspond to weakly-coupled quark-gluon plasma. Note that the nominal expectation is that $\rho(\lambda) \propto \lambda^3$ in UV ($\lambda \to \infty$) for all three phases due to asymptotic freedom.

The above is schematically represented by Fig. 2 (top horizontal line structure) where the order from left-to-right follows the case when transitions are due to increasing temperature (bottom line structure). Temperature T_{A} generically marks the crossover in Dirac spectral properties and this transition is thus on the same footing as the chiral crossover. Temperatures T_{IR} and T_{UV} mark transitions to IR and UV phases respectively.

The phase structure in the full set $\mathcal{T}$ of SU(3) gauge theories with fundamental quarks is schematically represented by Fig. 3 (left) [2]. Note that $\mathcal{T}$ is a multidimensional space (T, number of flavors N_f, individual quark masses) and only T and N_f have an explicit representation in Fig. 3 (left). The accumulated knowledge endowing the scheme with information is that the phase sequence $B \to IR \to UV$ (or any part of it) occurs not only via transitions due to increasing temperature, but also via increasing the number of flavors and via *decreasing* the individual quark masses m_i [1]. Important case is when IR phase arises from B phase at sufficiently large N_f by lowering the quark masses alone. In the degenerate near-massless case this situation is schematically shown in Fig. 3 (right), which for $T \to 0$ approaches what is known as the conformal window region [15].

[3]Note that the logarithmic IR behaviors, such as one predicted in low-temperature QCD by chiral perturbation theory [14], entail $p = 0$ and belong to B phase.

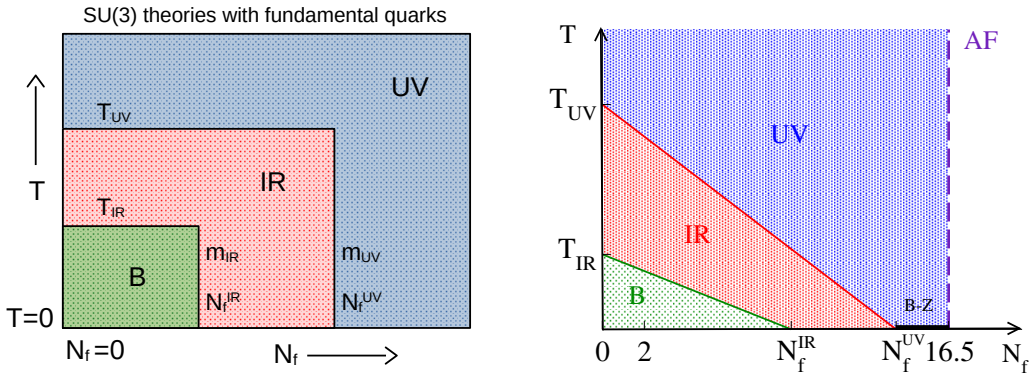

Figure 3: Left: schematic phase diagram of SU(3) gauge theories with fundamental quarks (set $\mathcal{T}$) based on the abundance of deep-IR degrees of freedom and IR scale invariance. Right: the case of near-massless quarks. The asymptotic freedom (AF) boundary is at $N_f = 16.5$. See the discussion in the text.

The corresponding transition parameters $N_f^{\rm IR}$ and $N_f^{\rm UV}$ delimit its strongly-coupled part [1] while theories in the regime $(N_f^{\rm UV}, 16.5)$ are expected to be governed by the weakly-coupled Banks-Zaks fixed point. Note that the straight-line phase boundaries in Fig. 3 simply signify the lack of detailed knowledge at present.

The important special case is the $T-m$ phase diagram of $N_f = 2$ (mass-degenerate) flavors or that for N_f = 2+1 theory with heavy quark held at the physical strange-quark mass. These are both very accurate and faithful approximations of "real-world QCD" when light-quark mass m is set to physical value. Varying m probes the effects of light quarks and the approach to the chiral limit. The simplest scenario for inclusion of IR phase is shown in Fig. 4 where the red solid line is the line of IR phase transitions starting at $m = 0$ with the chiral transition at T_c, passing through $T_{\rm IR}$ at the physical point, and ending at the Polyakov-line transition of pure-glue theory ($m = \infty$) denoted as T_c^{pg} here. Generic crossovers (e.g. the chiral one) are represented by the green dashed line, with $T_{\rm A}$ denoting the associated temperature.

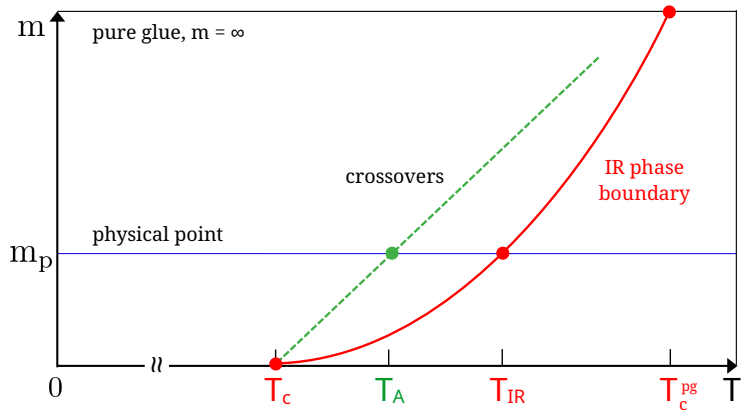

Figure 4: The conjectured $N_f = 2$ (or $N_f = 2+1$) thermal QCD phase diagram including the IR phase [1]. See e.g. the talk by I. Horváth at FunQCD22 workshop for one of the explicit mentions of this structure: https://drive.google.com/file/d/1vZ0AY0WsZAfF9iV7-Br-E_2NiwaZzRGp/view.

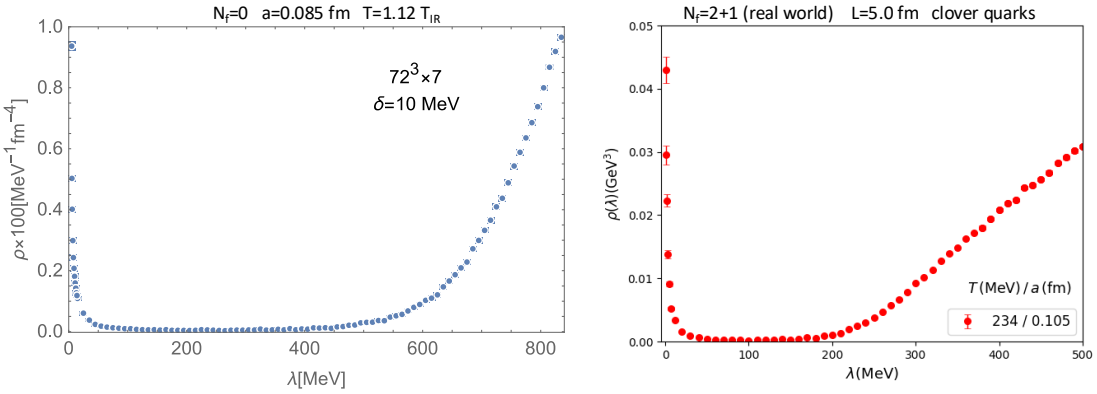

Figure 5: Dirac spectral densities for pure-glue QCD (left, [16]) and "real-world" ($N_f = 2+1$) QCD (right, [17]). The parameters of regularized systems in question are specified in the plots.

2.1 Some Key Evidences

The power of numerical lattice QCD lies, among other things, in the fact that by virtue of fully realizing a regularized system, it is able to verify any of its conjectured features. By the same token, it can also uncover qualitatively new aspects that were not even considered. The discovery of IR phase gives a relevant example of this. Indeed, it was widely expected that thermal fluctuations universally suppress IR dof's and Dirac spectrum was generally assumed to become IR-depleted upon the "QCD transition". Instead, the Fig. 5 shows the state of the art results for spectral densities of the overlap Dirac operator in pure-glue (left) and real-world (right) QCD, showing an entirely different IR world clearly emerging at large volumes when in the IR phase.

Two ingredients were of key relevance for the notion of IR phase to develop. The first one relates to the generic worry that what is observed on the lattice may be a regularization artifact that disappears in the continuum limit. This was resolved for pure-glue QCD in Ref. [2] and for "real-world" QCD ($N_f = 2+1$ at physical point) in Ref. [18]. Fig. 6 shows the UV cutoff dependences of mode abundance in the inner core of the IR peak. They reliably extrapolate to non-zero values. In the pure-glue case the plot shows the spectrum of the overlap Dirac operator while in $N_f = 2+1$ case that of the staggered operator governing the dynamics of lattice quarks.

The second key ingredient was the revelation that the unusual IR accumulation has a power-law

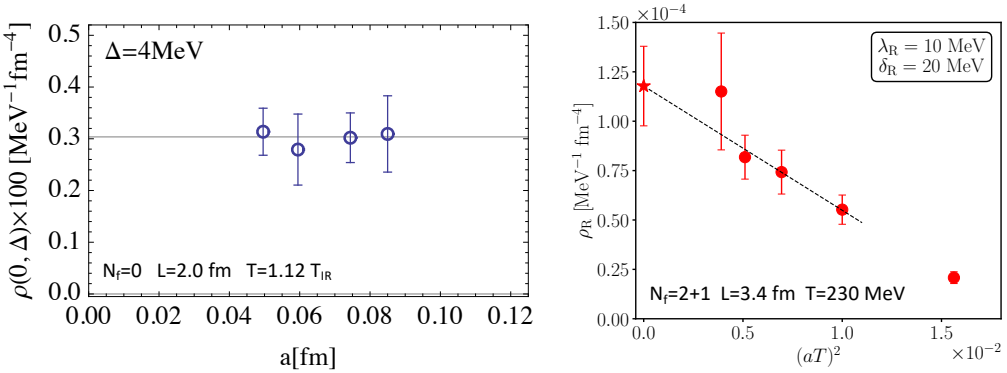

Figure 6: Scaling of the strength of IR peak in Dirac spectral densities for pure-glue QCD (left, [2]) and "real-world" QCD (right, [18]). The latter uses staggered dynamical lattice quarks.

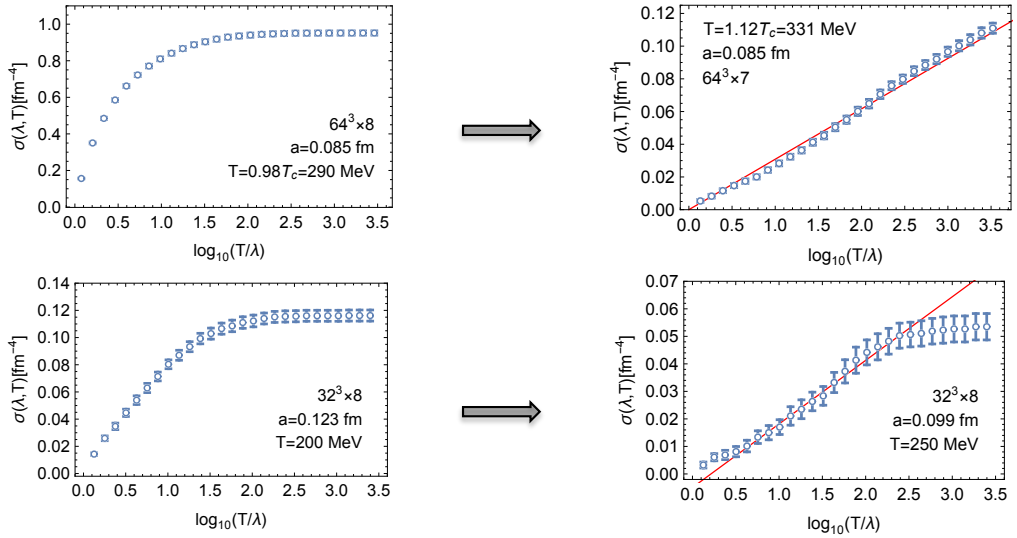

Figure 7: Transitions to IR phase in pure-glue (top) and "real-world" QCD (bottom) [1]. See the explanation in the text. Real-world QCD refers to $N_f = 2 + 1$ at physical point.

character. In particular, $\rho(\lambda)$ behaves in IR as a near-pure power λ^p with $p = -1 + \delta$ and $\delta > 0$ very small [1]. This is shown in Fig. 7 where the variables were chosen so that pure $p = -1$ corresponds to a rising straight line. In particular, $\sigma(\lambda, T)$ is a cumulative density for the interval (λ, T). Approaching deeper IR means moving to the right on the plots. Notice that in the pure-glue case the drastic change shown occurs when transiting from $T = 0.98 T_{\rm IR}$ to $T = 1.12 T_{\rm IR}$, and the power law in IR phase persists for over three orders of magnitude in scale. Temperature $T_{\rm IR}$ here coincides with T_c of Polyakov line phase transition [1]. The "real-world" case behaves very similarly at $T = 250$ MeV although the extent in scale is smaller due to smaller volumes.

2.2 Why IR and Why Phase?

The "IR" in IR phase arose from the qualitatively enhanced propensity of dof's to be arbitrarily infrared upon crossing into this new regime. The connection to IR fixed points associated with the conformal window offered itself naturally [1] although the details still need to be investigated. Most of the concluded features of the phase come from studies of thermal QCD, with temperature being the transition-inducing parameter. From the physics standpoint, this is arguably the most important setting to investigate in fact. At present, the best estimate for the value of $T_{\rm IR}$ in real-world QCD comes from $N_f = 2 + 1$ studies at physical quark masses and yield [1, 17, 18]

$$200 \text{ MeV} \ < \ T_{\rm IR} \ < \ 230 \text{ MeV} \tag{2}$$

The chiral crossover temperature $T_{\rm A} \to T_{\rm A}^c \approx 155$ MeV is well-known [19–21].

Several intriguing proposed features of the IR regime make it a phase in the conventional sense [1, 3, 4]. In particular, upon crossing into the IR phase the following occurs:

***(i)* IR-Bulk Separation.** The system becomes multicomponent with the IR segment decoupling and becoming an autonomous subsystem (independent component).

***(ii)* IR Scale Invariance.** Glue fields of the IR component become scale invariant (at least asymptotically in IR).

(iii) **Non-Analyticity.** Non-analytic behavior in Dirac spectral properties (in λ-dependence) appears and translates into non-analytic T-dependence of physical observables at the transition.

(iv) **Infinite Glue Screening Lengths.** Gluon fields start exhibiting long-range spatial correlations.

In the following section we will describe how these features interrelate with the existence of Anderson-like transitions in high-temperature QCD.

3. IR Phase and Anderson-like Localization

At the time the notion of IR phase was put forward in [1], some of the arguments for justification of properties ***(i)-(iv)*** already utilized the existence of the Anderson-like mobility edge $\lambda_{\rm A} > 0$ in Dirac spectra at high temperatures. When the metal-to-critical scenario utilizing also the new mobility edge at $\lambda_{\rm IR} = 0$ was put forward [3, 4] (see Sec. 1), essentially all proposed features of IR phase could be thought about under that umbrella. In this section we describe this ensuing relationship between the Anderson-like localization phenomena and thermal QCD.

3.1 Anderson Mobility Edges

Anderson localization is an old subject [5] that became quite vast in part due to the wealth of its applications [6]. For present purposes we only need a cursory knowledge of the topic, mostly embodied in the abstract notion of Anderson transitions or the associated critical points: the mobility edges. On one side of the transition are extended ("conducting") states while on the other side the exponentially localized ("insulating") ones. Transition occurs due to spatial disorder (e.g. random potentials), and the criticality at the edge is conveyed, among other things, by the fact that the density-density (probability-probability) spatial correlation length in modes diverges. Schematics of these transitions are shown in Fig. 8. For example, when approaching the mobility edge indicated by energy $E_{c1} > 0$ on the phase diagram (left plot) from the localized side $E > E_{c1}$, then the geometric scale ℓ (mode size, "localization length") associated with the mode varies as

$$\ell(E) \propto (E - E_{c1})^{-\nu} \propto \xi(E) \qquad \nu > 0 \tag{3}$$

and is proportional to the correlation length ξ. Directly at criticality, the density-density correlation function becomes long-range namely $L^6\langle p(r)p(r')\rangle \propto (|r-r'|/L)^{-\eta}$ in 3D (see e.g. [23]). Here $p(r) = \psi^\dagger\psi(r)$ with ψ the eigenstate.

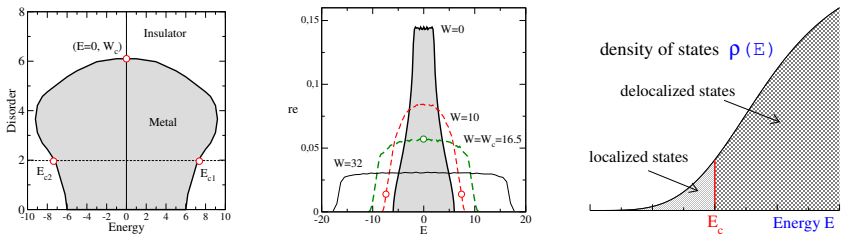

Figure 8: Generic schematics of Anderson transitions: phase diagram, density of states and the mobility edge. Courtesy of Peter Markoš and Ref. [22].

3.2 IR-Bulk Separation

The idea of IR-Bulk separation became suggestive after the striking bimodal structure of spectral densities became the fact of the continuum limit [2]. However, that in itself doesn't guarantee that the modes, and thus the physics itself, associated with spectral segments so separated are fully independent of one-another. One possibility that would make this very assuring is if e.g. $\rho(\lambda)$ had a region of full depletion ($\rho = 0$) between the two parts. While it is very possible that this does happen upon removing both the IR and UV cutoffs, it has not been verified in simulations yet.

But it is also not necessary. Indeed, a more general idea is that there is in principle a large class of spectral non-analyticities between IR and Bulk that may serve to indicate their decoupling. To that end, the original work [1] suggested that the previously seen [10, 11] Anderson-like mobility edge $\lambda_{\rm A} > 0$ perfectly fits the bill in terms of providing for the needed non-analytic arrangement. After all, it is a critical point ("phase transition" point) within the all-important Dirac substructure of QCD. As such, modes below and above $\lambda_{\rm A}$ do not talk to each other, especially when $\lambda_{\rm A}$ is truly Anderson-like when the expected nature of spatial correlations across the mobility edge conforms to that [6]. Thus, within the metal-to-critical picture of transition to IR phase the role of $\lambda_{\rm A}$ is to produce the IR-Bulk separation.

3.3 IR Scale Invariance and Infinite Glue Screening Lengths

In the proposal of IR phase [1], the chief motivation for IR scale invariance of glue was the near-pure power-law behavior of $\rho(\lambda)$. Indeed, in the spirit of the inverse scattering problem in quantum mechanics, this was suggested to be the result of scale invariance (in the statistical sense) of the underlying glue. Another motivation was that IR accumulation of Dirac modes similar to thermal case also occurred in the vicinity of conformal window as a result of lowering the quark mass [13, 24]. This then suggested the contiguous IR phase region in the theory space (see Fig. 3) and made IR scale invariance natural from that point of view.

The metal-to-critical scenario of transition to IR phase arranges for long-range correlations (power-law decays; infinite correlation lengths) via the strictly IR Anderson-like mobility edge $\lambda_{\rm A} = 0$ shown to be generated by QCD [3, 4]. Indeed, identifying the IR phase transition with the emergence of $\lambda_{\rm A}$ means that critical long-range correlations in deep-IR Dirac modes ensue immediately upon entering the phase. This then translates into long-range correlations in gluonic composite fields which can be scale-decomposed via these eigenmodes [25–27].

In this way, metal-to-critical scenario not only incorporates the infinite glue screening lengths and at least an asymptotic IR scale invariance of glue in the IR phase, but also provides for a concrete and (from the particle physics point of view) highly unusual mechanism of its genesis.

3.4 Non-Analyticity

True phase transitions are accompanied by the appearance of non-analyticities in the thermodynamic limit. Identifying them in transitions to IR phase went hand-in-hand with creating the metal-to-critical scenario as well [3, 4]. Indeed, the striking feature of Anderson transitions is the spatial dimensional collapse of states on the localized side. Given the appearance of Anderson-like mobility edges in IR phase, this aspect emerged naturally as a prime candidate for creating non-analyticities in the behavior of the partition function and the observables. But the formalization of

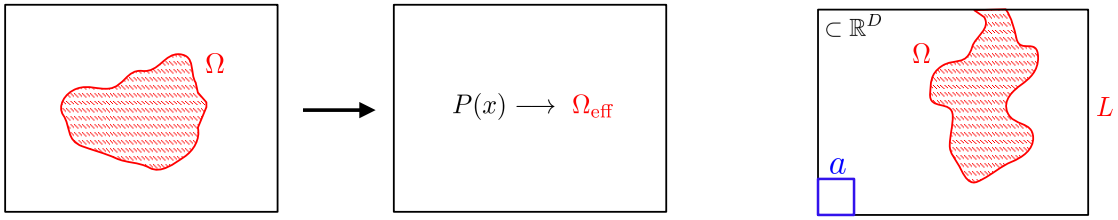

Figure 9: Left: Instead of the fixed subset Ω and its measure, Effective-Number Theory shows how to define the effective subset $\Omega_{\rm eff}$ from the underlying probability distribution $P(x)$. Right: IR dimension quantifies the change in the measure of the set Ω in response to change of IR cutoff L.

dimensional arguments happened to be a non-trivial task. Indeed, the notion of spatial dimension associated with Schrödinger eigenstates (or probability distribution in metric space more generally) didn't exist in the usual measure-based Hausdorff/Minkowski sense. This gap was filled by Effective-Number Theory [28] which constructed the needed effective counting measures (Fig. 9 left), and subsequently by Effective-Dimension Theory [29] which showed that these measures lead to a unique notion of effective dimension.

Noteworthy element here is that, rather than UV dimensions familiar from the analyses of fractal sets, it is the IR dimensions that are of prime interest here. IR dimensions are unconventional [29]: while the UV one gauges the response of measure to the decrease of UV cutoff a, IR dimension does that with the increase of IR cutoff L. More precisely, for the case of fixed sets and for the effective case of probability distributions we have respectively

$$N_+(\Omega,a,L) \propto L^{d_{\rm IR}(\Omega,a)} \quad \text{or} \quad \mathcal{N}_\star(P,a,L) \propto L^{d_{\rm IR}(P,a)} \quad \text{for} \quad L\to\infty \tag{4}$$

with schematics (the case of fixed set) shown in the right plot of Fig. 9. Note that N_+ is the number of elementary volume elements covering Ω at given a and L, while $\mathcal{N}_\star$ is the minimal effective count [28] of these elements given the $P(x)$ in question.

For QCD with its Dirac modes or Anderson models with their Schrödinger states, these dimensions have another of λ (Dirac scale) or E (energy) labels and spatial probability distributions are specified by modes/states themselves. Effective counts $\mathcal{N}_\star$ in the definition of $d_{\rm IR}$ are QCD/disorder averaged. Extensive calculations [3, 17, 30], suggest the spectral portrait of IR dimensions shown schematically in Fig. 10. While for $T < T_{\rm IR}$ one has the conventional $d_{\rm IR} = 3$ across the Dirac spectrum, in IR phase a pattern of discontinuities at mobility edges $\pm\lambda_{\rm A}$ and $\lambda_{\rm IR}$ appear. The most intriguing aspect is that at $\lambda_{\rm IR}$, exact zeromodes have $d_{\rm IR} = 3$ but arbitrarily close to criticality the dimension becomes $d_{\rm IR} = 2$. The relevant part of evidence for this is shown in Fig. 11 for both pure-glue [3] and $N_f = 2+1$ real-world QCD [17]. In the latter case the data nicely distinguishes the thermal state at $T = 187$ MeV below IR phase from that at $T = 234$ MeV in IR phase.

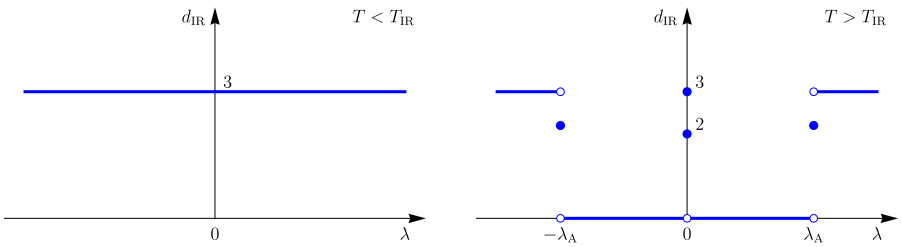

Figure 10: IR dimensions of QCD Dirac modes in the B phase (left) and in the IR phase (right) [30].

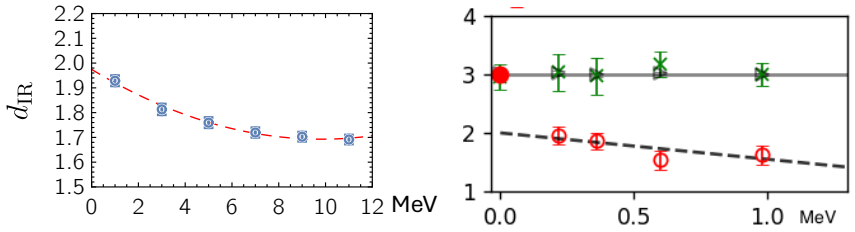

Figure 11: IR dimensions of near-critical near-zero modes in IR phase. On the x-axis is the width of the near-zero region. Left [3]: pure-glue QCD at $T = 0.12T_{\rm IR}$. Right [17]: $N_f = 2+1$ real-world QCD at $T = 234$ MeV (red) and at $T = 187$ MeV (green, outside of IR phase). Full symbols are exact zeromodes.

We emphasize that, given the singular accumulation of near-zero modes in IR phase, $d_{\rm IR} = 2$ actually dominates its deep-IR physics, and discontinuities of Fig. 10 will translate into various non-analyticities at $T_{\rm IR}$. For example, given the Dirac mode expansion of action density [25–27] the above results imply the T-dependence of $d_{\rm IR}$ for IR part of F^2 as shown in Fig. 12. Note that $d_{\rm IR} = 0$ for UV phase is an arbitrary definition since there are no IR modes.

4. Conclusions

In this talk I attempted to convey my view that, by virtue of the new IR phase, the phenomenon of Anderson-like localization has secured a very relevant place in the Standard Model of particle physics [4]. While a more precise relation between "Anderson and Anderson-like" is yet to be determined, it is clear that the ideas developed in the former context are very fruitful for building a detailed understanding of this new IR regime revealed by lattice QCD.

Finally, I wish to acknowledge few selected works, namely [31–34] which, one way or another, had the connection to the course of developments described here.

Acknowledgments

I enthusiastically acknowledge the long-term productive collaboration with Andrei Alexandru on the topics presented here. Extensive technical help from Dimitris Petrellis is also gratefully acknowledged. Hali, Sylvia and Vlado made this text possible. Thank you.

References

[1] Andrei Alexandru and Ivan Horváth. Possible New Phase of Thermal QCD. *Phys. Rev. D*, 100(9):094507, 2019.

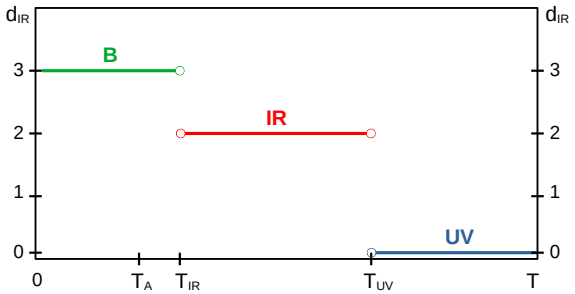

Figure 12: T-dependence of $d_{\rm IR}$ for deep-IR Dirac modes. It is also the spatial dimension of F^2 in IR regime.

[2] Andrei Alexandru and Ivan Horváth. Phases of SU(3) Gauge Theories with Fundamental Quarks via Dirac Spectral Density. *Phys. Rev.*, D92(4):045038, 2015.

[3] Andrei Alexandru and Ivan Horváth. Unusual Features of QCD Low-Energy Modes in the Infrared Phase. *Phys. Rev. Lett.*, 127(5):052303, 2021.

[4] Andrei Alexandru and Ivan Horváth. Anderson metal-to-critical transition in QCD. *Phys. Lett. B*, 833:137370, 2022.

[5] P. W. Anderson. Absence of diffusion in certain random lattices. *Phys. Rev.*, 109:1492–1505, Mar 1958.

[6] Elihu Abrahams. *50 Years of Anderson Localization*. WORLD SCIENTIFIC, 2010.

[7] Adam Miklos Halasz and J. J. M. Verbaarschot. Universal fluctuations in spectra of the lattice Dirac operator. *Phys. Rev. Lett.*, 74:3920–3923, 1995.

[8] Antonio M. Garcia-Garcia and James C. Osborn. Chiral phase transition and anderson localization in the instanton liquid model for QCD. *Nucl. Phys. A*, 770:141–161, 2006.

[9] Antonio M. Garcia-Garcia and James C. Osborn. Chiral phase transition in lattice QCD as a metal-insulator transition. *Phys. Rev. D*, 75:034503, 2007.

[10] Tamas G. Kovacs and Ferenc Pittler. Anderson Localization in Quark-Gluon Plasma. *Phys. Rev. Lett.*, 105:192001, 2010.

[11] Matteo Giordano, Tamas G. Kovacs, and Ferenc Pittler. Universality and the QCD Anderson Transition. *Phys. Rev. Lett.*, 112(10):102002, 2014.

[12] Laszlo Ujfalusi, Matteo Giordano, Ferenc Pittler, Tamas G. Kovács, and Imre Varga. Anderson transition and multifractals in the spectrum of the Dirac operator of Quantum Chromodynamics at high temperature. *Phys. Rev. D*, 92(9):094513, 2015.

[13] Andrei Alexandru and Ivan Horváth. Chiral Symmetry Breaking and Chiral Polarization: Tests for Finite Temperature and Many Flavors. *Nucl.Phys.*, B891:1–41, 2015.

[14] J. C. Osborn, D. Toublan, and J. J. M. Verbaarschot. From chiral random matrix theory to chiral perturbation theory. *Nucl. Phys.*, B540:317–344, 1999.

[15] Tom Banks and A. Zaks. On the Phase Structure of Vector-Like Gauge Theories with Massless Fermions. *Nucl. Phys.*, B196:189–204, 1982.

[16] Andrei Alexandru and Ivan Horváth. 2023, unpublished.

[17] Xiao-Lan Meng, Peng Sun, Andrei Alexandru, Ivan Horváth, Keh-Fei Liu, Gen Wang, and Yi-Bo Yang. Separation of Infrared and Bulk in Thermal QCD. *JHEP*, 2024(12):101, 2024.

[18] Andrei Alexandru, Claudio Bonanno, Massimo D'Elia, and Ivan Horváth. Dirac spectral density in Nf=2+1 QCD at T=230 MeV. *Phys. Rev. D*, 110(7):074515, 2024.

[19] Y. Aoki, G. Endrodi, Z. Fodor, S.D. Katz, and K.K. Szabo. The Order of the quantum chromodynamics transition predicted by the standard model of particle physics. *Nature*, 443:675–678, 2006.

[20] Y. Aoki, Szabolcs Borsanyi, Stephan Durr, Zoltan Fodor, Sandor D. Katz, Stefan Krieg, and Kalman K. Szabo. The QCD transition temperature: results with physical masses in the continuum limit II. *JHEP*, 06:088, 2009.

[21] A. Bazavov et al. Chiral crossover in QCD at zero and non-zero chemical potentials. *Phys. Lett. B*, 795:15–21, 2019.

[22] P. Markoš. Numerical analysis of the anderson localization. *Acta Physica Slovaca*, 56(5):561–685, Oct 2006.

[23] Ferdinand Evers and Alexander D. Mirlin. Anderson transitions. *Reviews of Modern Physics*, 80(4):1355–1417, Oct 2008.

[24] Andrei Alexandru and Ivan Horváth. Broken Valence Chiral Symmetry and Chiral Polarization of Dirac Spectrum in N_f=12 QCD at Small Quark Mass. *AIP Conf. Proc.*, 1701(1):030008, 2016.

[25] Ivan Horváth. Coherent lattice QCD. *PoS*, LAT2006:053, 2006.

[26] Ivan Horváth. A Framework for Systematic Study of QCD Vacuum Structure II: Coherent Lattice QCD. 2006.

[27] Andrei Alexandru, Ivan Horváth, and Keh-Fei Liu. Classical Limits of Scalar and Tensor Gauge Operators Based on the Overlap Dirac Matrix. *Phys.Rev.*, D78:085002, 2008.

[28] Ivan Horváth and Robert Mendris. Effective Number Theory: Counting the Identities of a Quantum State. *Entropy*, 22:1273, 2020.

[29] Ivan Horváth, Peter Markoš, and Robert Mendris. Counting-Based Effective Dimension and Discrete Regularizations. *Entropy*, 25(3):482, 2023.

[30] Andrei Alexandru, Ivan Horváth, and Neel Bhattacharyya. Localized modes in the IR phase of QCD. *Phys. Rev. D*, 109(1):014501, 2024.

[31] Robert G. Edwards, Urs M. Heller, Joe E. Kiskis, and Rajamani Narayanan. Chiral condensate in the deconfined phase of quenched gauge theories. *Phys.Rev.*, D61:074504, 2000.

[32] Viktor Dick, Frithjof Karsch, Edwin Laermann, Swagato Mukherjee, and Sayantan Sharma. Microscopic origin of $U_A(1)$ symmetry violation in the high temperature phase of QCD. *Phys. Rev.*, D91(9):094504, 2015.

[33] Robin Kehr, Dominik Smith, and Lorenz von Smekal. QCD Anderson transition with overlap valence quarks on a twisted-mass sea. 4 2023.

[34] Tamas G. Kovacs. Fate of Chiral Symmetries in the Quark-Gluon Plasma from an Instanton-Based Random Matrix Model of QCD. *Phys. Rev. Lett.*, 132(13):131902, 2024.